Journal of Materials Chemistry B

Accepted Manuscript

ROYAL SOCIETY OF CHEMISTRY

www.rsc.org/materialsB

Journal Name

RSCPublishing

ARTICLE

Nanocomposited Silicone Hydrogels with a Laser-assisted Surface Modification for Inhibiting the Growth of Bacterial Biofilm

Cite this: DOI: 10.1039/x0xx00000x

Received 00th January 2012,
Accepted 00th January 2012

DOI: 10.1039/x0xx00000x

www.rsc.org/

P. Yin,[a] G. B. Huang,[a] W. H. Tse,[b] Y. G. Bao,[c] J. Denstedt,[c] and J. Zhang [a,b*]

Surface and interface modifications of synthetic silicone hydrogels used for wearable and implantable medical devices, e.g. catheter, contact lenses, are critical to overcome their poor mechanical properties and biofouling. In this paper, silica nanoparticles (SiO_2 NPs) were incorporated within silicone hydrogels through photo-polymerization. As compared to the silicone hydrogel, the nanocomposited silicone hydrogel shows highly textured microstructures, increased swelling behaviour, and improved stiffness. Meanwhile, a hydrophilic surface of silicone hydrogel is important to minimize protein fouling which forms conditioning layer for the growth of bacterial biofilm. Here, we applied a matrix-assisted pulsed laser evaporation (MAPLE) with a pulsed Nd:YAG Laser at 532 nm to deposit polyethylene glycol (PEG) on the surface of the nanocomposited silicone hydrogels. The PEG deposited on the nanocomposited silicone hydrogels forms islands at submicron-scale which increase with increasing irradiation time (t). The protein adsorption on nanocomposited silicone hydrogel with PEG deposition decreases over 40 ± 2 % when t = 2hr. Compared to the commercial silicone catheters, the nanocomposited silicone hydrogel with PEG deposition can reduce the growth of bacteria from $1.20x10^6$ CFU/cm^2 to $3.69x10^5$ CFU/cm^2. In addition, the relative cell viabilities of NIH/3T3 mouse fibroblast cells treated by the nanocomposited silicone hydrogels coated with/without PEG were studied. No toxic effect is imposed on the cells. Consequently, MAPLE process is a controllable, contamination-free technique to modify the surface of silicone hydrogels. We expect that the nanocomposited silicone hydrogels with proper surface treatment can be applied in various wearable and implantable medical devices.

Introduction

Biofilms are multispecies communities of microorganisms. *Escherichia coli* (*E.coli*) and *Enterococcus* species are dominant pathogens.[1-2] Over 65% bacterial-related infections are associated with the growth of bacterial biofilms on medical devices used for orthopaedics, catheters, contact lenses, vascular stents.[3-4] It is quite costly and inconvenient to repair or replace the bio-fouled medical devices. Moreover, the frequent invasive-surgeries or procedures due to the limited clinical lifetime of medical devices may lead to the increased risk of developing serious diseases or even death. It has been known that the formation of bacterial biofilms starts with the adhesion of protein layers, that is, the "conditioning film", in which bacteria have developed into organized communities with different functions.[5-6] Sessile bacterial cells release antigens and stimulate the production of antibodies within biofilms, which normally cause immune complex damage to the surrounding tissue.[5-7] Therefore, it is crucial to design the next-generation biomedical devices that can inhibit the growth of biofilms.

Silicone hydrogels have been applied in various medical devices, including contact lenses, catheters, and ureteral stents because of their good biocompatibility and high oxygen permeability.[8-9] However, high protein adsorption on silicone hydrogel are easily happened, which could be caused by its hydrophobic components, i.e. siloxane group. Interpenetrating polymer network (IPN) has been applied to improve the hydrophilic properties of silicone hydrogel. For instance, hydrophilic monomer, such as (N,N-dimethylacrylamide, DMA), is introduced into 3-methacryloxypropyltris-trimethylsiloxy-silane (TRIS) and silicone macromer.[12] Recently, IPN organic-inorganic nanocomposites by incorporating inorganic nanostructured fillers into organic matrices show enhanced properties while maintaining the chemical and physical properties of inorganic nanoparticles and

polymer networks.[13-14] Different methods have been exploited to overcome the thermodynamic and kinetic barriers in incorporating hydrophilic inorganic nanoparticles into hyodrophobic polymeric matrix. For instance, solvent-exchange processing for high-performance elastomeric nanocomposites by introducing silica nanoparticles (SiO_2 NPs) into elasthane polyetherurethane.[15-16] Here, we applied the photo-polymerization to form the nanocompoisted silicone hydrogel through incorporating SiO_2 NPs into the silicone hydrogel. SiO_2 NPs are translucent hydrophilic nanomaterials. Silanol (Si-OH) is normally formed on the surface of SiO_2 NPs, which is able to lead to versatile chemical reactions.[17-18]

In addition, physical and chemical methods have been applied to passively and/or actively prevent bio-fouling on biomedical devices.[10-11] Polyethylene glycol (PEG), a polyether, has been used to modify the surface of polymers to reduce protein adhesion due to its hydrophilic properties.[19-20] The conventional wet chemical methods used for complex organic molecule deposition include dip coating and spin coating.[21-22] For precisely controlling the deposition, and, minimizing the contamination caused by additional organic regents in wet chemical process, physical vapour deposition may provide an alternative solution for modifying silicone surface with hydrophilic molecules.

Matrix-assisted pulsed laser evaporation (MAPLE), a modification of the pulsed laser deposition (PLD) technique, was developed to ensure retention of the properties and structures of deposited organic molecules.[23-24] In MAPLE process, the targeted materials/molecules are normally embedded in frozen solvents. The energy of the laser is mostly absorbed by the solvent to reduce the damage to the target molecules. Excimer lasers or Nd: YAG lasers with the second or third harmonics are normally used for MAPLE processes; infrared laser sources are utilized in particular cases.[25] Here, we applied MAPLE process to deposit PEG on nanocomposited silicone hydrogels with different irradiation time (*t*).

In this paper, the mechanical properties and protein absorption of the nanocomposited silicone hydrogels were investigated in comparison with the silicone hydrogel. Meanwhile, the capabilities of nanocomposited silicone hydrogels with/without PEG modification in inhibiting the growth of bacteria were studied. The cytotoxicity of the nanocomposited silicone hydrogels with/without PEG was further evaluated by using NIH/3T3 mouse fibroblast cell line.

Materials and methods

Materials

All chemicals used in this paper were purchased from Sigma-Aldrich (Ontario, Canada), including 3-aminopropyltriethoxysilane (APTS), tetra ethyl orthosilicate (TEOS), 3-(Trihydroxysilyl) propyl methyl phosphonate monosodium (TPMPH), and centrimonium bromide (CTAB), fluorescein isothiocyanate (FITC) which were encapsulated into SiO_2 NPs, and chemicals used for producing silicone hydrogel: 3-methacryloxypropyl tris (trimethylsiloxy) silane (TRIS), N,N-Dimethylacrylamide (DMA), N-vinylpyrolidinone (NVP), and ethylene glycol dimethacrylate (EGDMA), and the macromer bis-alpha,omega-(methacryloxypropyl) polydimethylsiloxane (Mw 7152), and polyethylene glycol (EG) used to modify the surface of hydrogels.

Synthesis of silica nanoparticles

Similar to our previous reports,[18, 26] a condensation and polymerization of TEOS was processed for producing SiO_2 NPs. 0.1 g CTAB was dissolved in 50 mL distilled deionized water at 80°C. 350 µL of 2M NaOH was added in the solution as catalyst to hydrolysis and condensation of the silica polymerization. Meanwhile, 5.5 mg FITC and 12 µL APTS were mixed in 3 mL of ethanol under dry nitrogen. Following that, the FITC-APTS solution and 350 µl of TEOS were added drop-wisely in CTAB solution. After 15 min's stirring, 127 µL of TPMPH was added and stirred for 2 additional hours. Nanoparticles were harvested and purified by sonification and centrifugation with ethanol at 8000 rpm. The product was washed by water/acetone/ethanol three times. Finally, the nanoparticles were freeze-dried and stored.

Synthesis of Nanocomposited Silicone Hydrogel

A photopolymerization process was applied in producing nanocomposited silicone hydrogel.[27] Briefly, 3 ml of a mixture of tris(hydroxymethyl)aminomethane) (TRIS), bis-alpha,omega-(methacryloxypropyl) polydimethylsiloxane, and

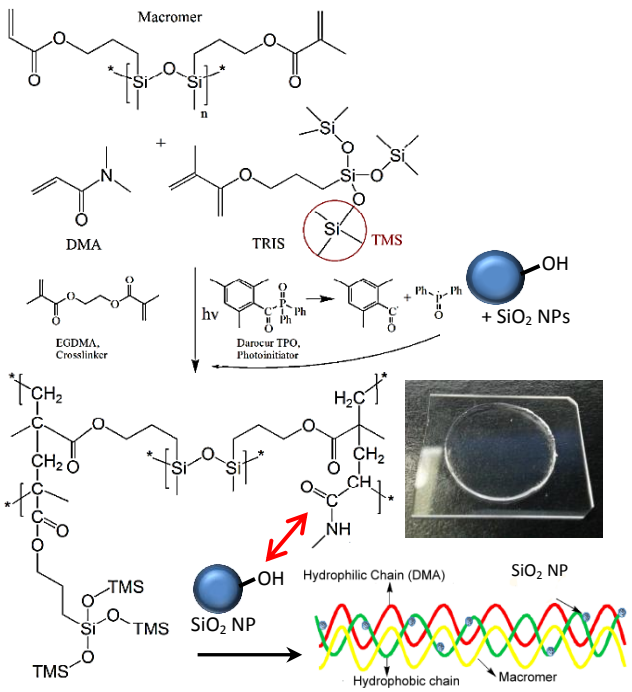

Scheme 1. Nanocomposited Silicone hydrogels made through a photopolymerization. The small inset photo shows the transparent nanocomposited silicone hydrogel on a glass slide.

DMA with a calculated volume ratio (4:1:2) was mixed with

0.18 ml NVP, 15 ml EGDMA and 0.3 ethanol. The mixture was then purged with dry nitrogen for 15 min, prior to the addition of 8 mg of photoinitiator (Diphenyl (2,4,6-trimethylbenzoyl) phosphine oxide) and stirred for 5 min. In addition, SiO_2 NPs suspended in 0.1mL ethanol was added to the above silicone polymer solution at a weight ratio of 1:200 prior to nitrogen purging and photopolymerization as shown in Scheme 1. This is the maximum weight ratio of SiO_2 NPs to a hydrogel matrix to maintain good light transmission.[28] The mixture was irradiated for 50 min by UV for complete crosslinking. The nanocomposited hydrogel was washed with ethanol and dried in air overnight.

Surface Modification through MAPLE Process

Scheme 2 indicates the surface modification by using MAPLE (PVD Products Inc.). PEG was diluted in isopropanol (12mL) with a concentration of 0.5 wt%. The mixture is transferred to the target holder which is cooled by liquid nitrogen. A Nd:YAG pulsed laser with the wavelength (λ) at 532 nm (Continuum, 20 Hz, 95 mJ/pulse) was used to irradiate the frozen target for one and two hours, respectively. The spot size of the laser beam is around 2.0 mm in diameter. The pressure of deposition chamber is about 1×10^{-6} Torr. The nanocomposited silicone hydrogel is used as the substrate. The substrate-to-target distance is 6 cm.

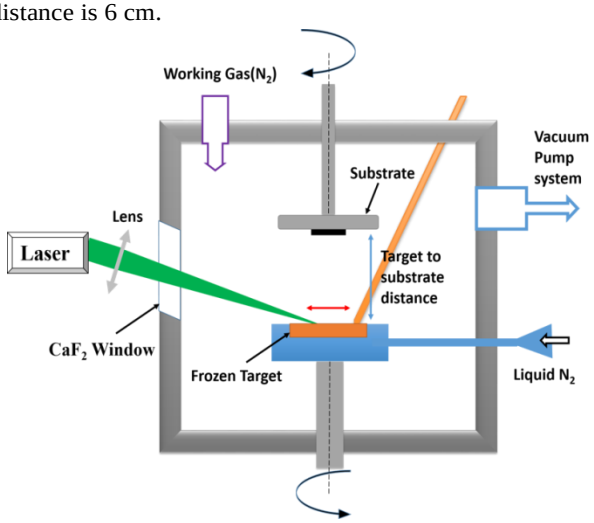

Scheme 2. Illustration of MAPLE process for depositing PEG on nanocomposited silicone hydrogels

Materials characterization

Transmission electron microscopy (TEM, Phillips CM10) was applied to study the microstructures of SiO_2 NPs. The diameter of the nanospheres were analyzed with ImageJ software (National Institutes of Health, USA) with an ANOVA and Kruskal-Wallis ($p<0.0001$). In addition, the nanocomposited silicone hydrogels with and without PEG coating were characterized by fourier transform infrared spectroscopy (FTIR), Scanning electron microscopy (SEM, Hitachi 3400s), and atomic force microscopy (AFM). Meanwhile, FITC loaded SiO_2 NPs (FITC-SiO_2 NPs) were produced using the same sol-gel process to study the dispersion of SiO_2 NPs in silicone network. Photoluminescence (PL) of FITC-SiO_2 NPs and silicone hydrogel incorporating with FITC-SiO_2 NPs were measured by a fluorometer (Photon Technology International (PTI-Horiba), London, Ontario, Canada). Fluorescence lifetimes of both FITC-SiO_2 NPs and silicone hydrogel incorporating with FITC-SiO_2 NPs were measured by the TM-30 Laser Strobe time-resolved fluorometer (Photon Technology International (PTI-Horiba), London, Ontario, Canada). The light source is a pulsed dye laser pumped by a pulsed nitrogen laser with the dye wavelength set at 480 nm (the bandwidth of the dye laser output is about 0.04 nm). Furthermore, there was a 525 nm long-pass filter used on the emission side so that no excitation light can enter the detector, that is, the scattering effect is ruled out. The PTI-patterned Strobe technique measures fluorescence decay curves (i.e. fluorescence intensity as a function of time) directly. It is considered a faster measurement than TCSPC (Time -Correlation Single Photon Counting) by using a non-linear detection timescale to record the fluorescence intensity.[29] The data analysis was performed with Felix GX analytical software package using a 1-to-4 exponential fitting function by chi-square minimization employing Marquardt-Levenberg algorithm with iterative reconvolution. In order to carry out reconvolution, an instrument response function (IRF) was measured by using a scattering suspension of Ludox in deionized water. For double exponential PL decays the intensity-weighed average lifetimes were calculated using the following equation.[30]

$$\tau_{ave} = \sum a_i \tau_i^2 / \sum a_i \tau_i \,, \qquad (1)$$

where a_i is the pre-exponential weight and τ_i the decay times obtained in the multi-exponential fitting.

Swelling behaviour

Swelling behaviour of silicone hydrogel and nanocomposited silicone hydrogel were evaluated. Samples were freeze-dried for 24 hours (h) to eliminate water content. Triplicated experiments were performed in deionized water at room temperature for 20 h in total. The swelling ratio was calculated as follows:

$$S = \frac{W_w - W_D}{W_D} * 100\% \qquad (2)$$

W_W and W_D are the weight of the swollen hydrogel and its corresponding dried weight, respectively. W_w was measured when samples were soaked in water for 0.5hr, 1hr, 2hr, 4hr, 8hr, and 20hr, respectively. Three repetitions were performed for all samples.

Mechanical properties

Specimens (1.0 x 1.0 cm^2) of the nanocomposite and plain hydrogel were mounted in a BioTester 5000 test system (CellScale Biomaterials Testing, Waterloo, Ontario). The specimens were stretched uniaxially with a load of 2 mN applied consistently during the tensile test. Meanwhile, the images of the deformation of the specimens were captured using a 1280x960 pixel charge coupled device CCD- camera.

The stress and strain produced in order to study the stress-strain curves of different samples and their Young's modulus (E) is described below.

$$E = \frac{Stress}{Strain} = \frac{\sigma}{\varepsilon} = \frac{\frac{F}{A}}{\frac{\delta L}{L_0}}, \quad (3)$$

where E is the Young's modulus in Pascal (Pa), F the force applied in Newton (N), the original cross-sectional area (A) through which the force was applied in metres squared (m^2), the displacement (δL) of the materials in meters (m), and the original length (L_0) of the materials.

Protein adsorption

Silicone samples with the same size (2.5 x 2.5 cm^2) were immersed in 0.5 mg/ml bovine serum albumin (BSA) in phosphate buffered saline (PBS) solution for 3 h at 37 o C. After that, the samples were rinsed with PBS solution to remove non-adsorbed BSA. After that, samples were then immersed in a PBS buffer with 1% sodium dodecyl sulfate (SDS) and sonicated for 20 min to completely detach BSA from the hydrogels. The BCA protein assay kit (Micro BCA™ Protein Assay Kit, Thermo Scientific, USA) was used to determine the protein concentration in the SDS-PBS solution with a UV-visible plate reader at a wavelength of 562 nm.

Antimicrobial efficiency

Antimicrobial efficiency of the nanocomposited silicone hydrogels with and without PEG coating were evaluated by using gram-positive bacterium, *S. aureus* (ATCC) and gram-negative bacteria, *E. coli* (strain W3110, ATCC), respectively. Using *E. coli* BL21 as an example, we applied the drop-test method in studying the growth of *E. coli* on synthetic silicone hydrogel and nanocomposited silicone hydrogel with and without PEG coating.[31] Samples (1cm × 1cm) were placed into sterilized 90-mm Petri dishes. Meanwhile, a glass slide is used as the control sample. *E. coli* (strain W3110) suspended in 100 µl PBS with a concentration of10^6 CFU/ml were dropped onto the surface of each sample. The samples were laid at room temperature in different time periods (i.e. 1, 2, 3, 4 hours). After each time period, the bacteria containing drops were washed from the sample surfaces using 5 ml PBS in the sterilized Petri dish. Then 10 µl of each bacteria suspension was spread on the LB Agar plate. The number of surviving bacteria was counted after incubation for 24 h at 37°C. The relative viability of *E.coli* was calculated, which is the counted number of sample plate divided by the counted number of control plate. The experiment was repeated 5 times.

Anti-bacterial efficiency of the developed nanocomposited silicone hydrogel was evaluated further in comparison with that of hydrogel-coated silicone Foley catheters (Biocath, CR Bard, Inc. Covington, GA, USA). *E.coli* C1214 were cultured with silicone hydrogel, nanocomposited silicone hydrogel, PEG coated nanocomposited silicone hydrogel, and silicone Foley catheter, respectively. All samples were cut into pieces with the same surface area (1.0x1.0 cm^2). Samples were incubated in 6 mL LB broth containing 6ul of fresh overnight *E.coli* C1214 cultures in 6-well plates. The plates were placed in a shaking incubator at 37°C at 100 rpm. After 24 hours, materials were removed and washed twice in sterile PBS solution to remove loosely associated organisms, and the adherent bacteria were removed by sonication for 10 minutes (Bransonic) in 1 mL of PBS, and vortexed for 1 minute. The solution was serially diluted and plated for CFU counts. 24 samples for each type of materials were tested. Both single and double student T-tests are applied in statistic study.

Cytotoxicity

50,000 NIH/3T3 mouse fibroblast cells were seeded into a 24 well culture plate and incubated in a 5% CO2 incubator overnight. Hydrogels and nanocomposites were cut into 0.5 g pieces and incubated with cells for 24 hours. Cell viability was accessed by using a 3-(4,5-Dimethylthiazol-2-yl)-2,5-diphenyltetrazolium bromide (MTT) Assay. Briefly, after remove the samples, the MTT reagent was added to 24-well plate and incubated at 37 ^oC for another 4hr, then DMSO was added to dissolve the purple formazan product. The resulting signals were measured at an absorbance of 490 nm.

Results and Discussion

Characterization of silicone hydrogel with/without SiO_2 NPs

The cross-sectional microstructures of the silicone hydrogel and the nanocomposited silicone hydrogel were examined by SEM. The polymer fibrils exist in both of the hydrogel and its nanocomposites due to monomer and macromer crosslinking as shown in Figure 1a &1b. While, the textures are more regular

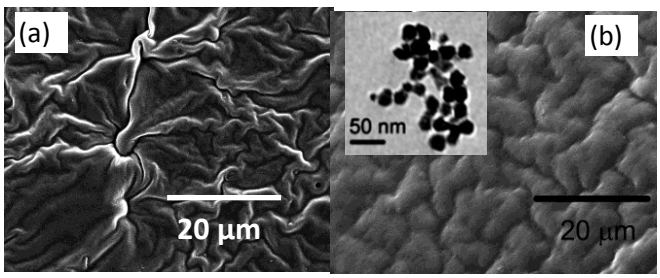

Figure 1. Cross-sectional SEM micrograph of (a)silicone hydrogel and (b) nanocomposited silicone hydrogel. The small inset image is the TEM micrograph of SiO_2 NPs.

for nanocompoisted silicone hydrogel, which could indicate the homogeneous dispersed SiO_2 NPs in silicone hydrogel network. The small inset in Figure 1b is the TEM micrograph of SiO_2 NPs which is estimated at 35±5 nm in diameter.

To further understand the dispersion of SiO_2 NPs in silicone hydrogel, we also produced FITC loaded SiO_2 NPs (FITC-SiO_2) using the same method.[18] Figure 2 displays the PL spectra of FITC-SiO_2 NPs and silicone hydrogel incorporated with FITC-SiO_2 NPs. As compared to the PL spectrum of FITC-SiO_2 NPs, a 3 nm-blue-shift is observed when FITC-SiO_2 NPs are dispersed within hydrogel as shown in figure 2(a). The

slight blue-shift is caused when a fluorophore is transferred from water, a polar solvent, to the silicone hydrogel, less polar matrix, the energy difference between the excited state and the ground state is increased due to the inability of the non-polar environment to stabilize the excited state. Furthermore, the calculated average lifetime of FITC-SiO_2 NPs in water and in silicone hydrogel is the same value (τ_{ave} = 3.8 ns). It indicates that the FITC-SiO_2 NPs homogenously incorporate within silicone hydrogel.

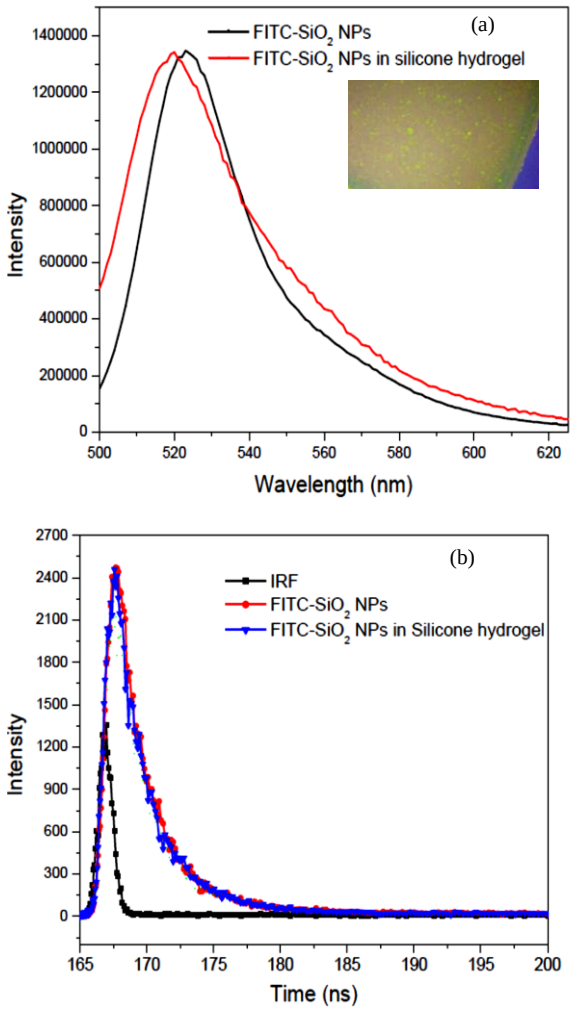

Figure 2. (a) Photoluminescence spectra of FITC-SiO_2 NPs and silicone hydrogel incorporating with FITC-SiO_2 NPs. A small inset is the photo of fluorescent silica nanoparticles dispersed in silicone hydrogel. (b) Time-resolved fluorescence measurements, IRF: instrument response function.

Figure 3 displays the swelling behaviours of the silicone hydrogel and the nanocomposited silicone hydrogel in water. The samples soaked in water for 0.5hr, 1hr, 2hr, 4hr, 8hr, and 20hr were weighed. The capability for absorbing water to the silicone hydrogel and the nanocomposited silicone hydrogel is approaching to the saturation at 20hr with weight-gaining around 20±2% and 26±3%, respectively. Clearly, the nanocomposited silicone hydrogel intends to absorb more water compared to the silicone hydrogel. The addition of DMA makes the silicone network partially hydrophilic.[27] Silanol (Si-OH) on the surface of SiO_2 NPs is able to covalently bind to DMA in silicone network homogenously, leading to the enhanced hydrophilic properties and swelling behaviours.

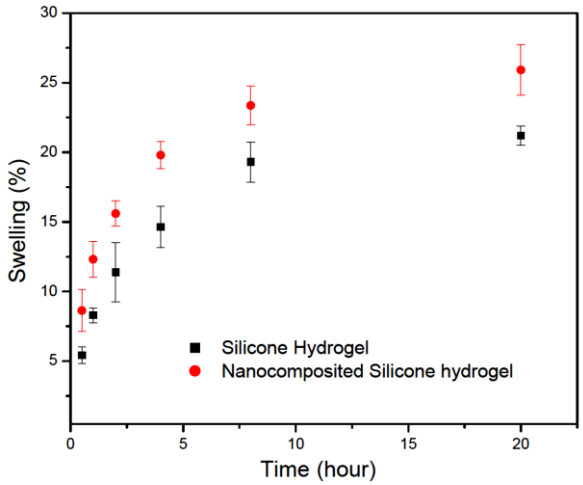

Figure 3. Swelling behaviors of silicone and nanocomposited silicone hydrogels.

In addition, proper mechanical stiffness is required for wearable and implantable medical devices, e.g. contact lens, catheters. Different body implants require different mechanical strengths. For example, bone implants require rigid materials, while skin wound covers require soft, tensile materials. Tensile modulus, also known as Young's modulus, of the hydrogel was measured. Young's modulus is a measure of the stiffness of a material, i.e., the higher the Young's modulus of a material, the stiffer it is, and the less strain it exhibits for a given stress.

The tensile modulus of silicone hydrogels and the nanocomposited silicone hydrogel (the weight ratio of SiO_2 NPs to silicone hydrogel = 1:200) were tested uniaxially. The calculated Young's modulus (E) of the nanocomposited silicone hydrogel increases over 12.9% from 0.62±0.02 MPa to 0.70±0.02 MPa as compared to that of the silicone hydrogel. The nanocomposited hydrogel has a similar Young's modulus with soft tissues in the range of 0.5 to 0.85 MPa.[32]

Characterization of PEG modification

The topography of nanocomposited silicone hydrogels with PEG deposition by MAPLE process was examined by AFM. As shown in Figure 4, island-shaped structures made of PEG molecules are deposited on the substrate. The PEG coatings are denser with increasing laser irradiation time (t). The PEG islands on the substrate have a diameter of approximately 0.7 µm and height of about 33.3 nm when t = 1hr; whereas the average size of PEG islands grows from 0.7 µm to nearly 2.5 µm, with a maximum height of approximately 115 nm when t = 2hr. PEG molecules formed islands rather than films on the substrate which is helpful to maintain the good oxygen permeability of silicone. The silicone and nanocomposited silicone hydrogels with/without PEG modification (t = 2hr) were examined by FTIR. Silicone and nanocomposited silicone hydrogels show identical peaks as shown in Figure 5a. Si – O – Si stretching (1040 cm^{-1}) can be recognized in the spectra.

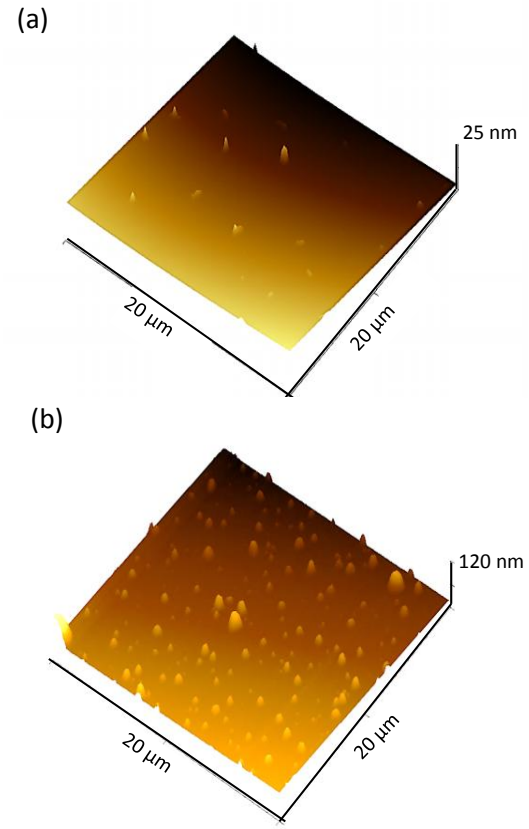

Figure 4. Topographies of PEG molecules coated on the substrate when (a) t = 1hr, (b) t = 2hr.

Furthermore, the typical $-CH_3$ stretch can be found near 2930 cm^{-1}, C-O, C=O, and -COO- stretching peaks can be observed in the region of 1200-1700 cm^{-1}. No -OH stretching peaks can be observed. The results suggest SiO_2 NPs with silanol (-Si-OH) functional group covalently bind to DMA in silicone network. Whereas the -OH stretching peaks at 3344 cm^{-1} and 3358 cm^{-1} appear when PEG molecules are deposited on both of silicone and nanocomposited silicone hydrogels as shown in Figure 5b. We also compare the FTIR spectrum of the nanocomposited silicone hydrogel with PEG deposited by MAPLE process to that of the nanocomposited hydrogel with PEG deposited by dip-coating. The FTIR spectra of silicone samples with PEG modification are quite similar as shown in Figure 6b. The results indicate that PEG can be successfully deposited on substrate by the MAPLE process with a pulsed Nd:YAG Laser at 532 nm without altering the molecular structures. It is also noted that PEG can be deposited by MAPLE process with a pulsed laser at 355 nm in which water or DMSO was used as a solvent.[33-34]

Protein absorption and bacterial growth

The protein adsorption property of silicone and nanocomposites were assessed by quantifying BSA adsorbed on the surface of samples by the Micro BCA™ Protein Assay Kit. Figure 6 shows the BSA adsorption on the nanocomposited silicone

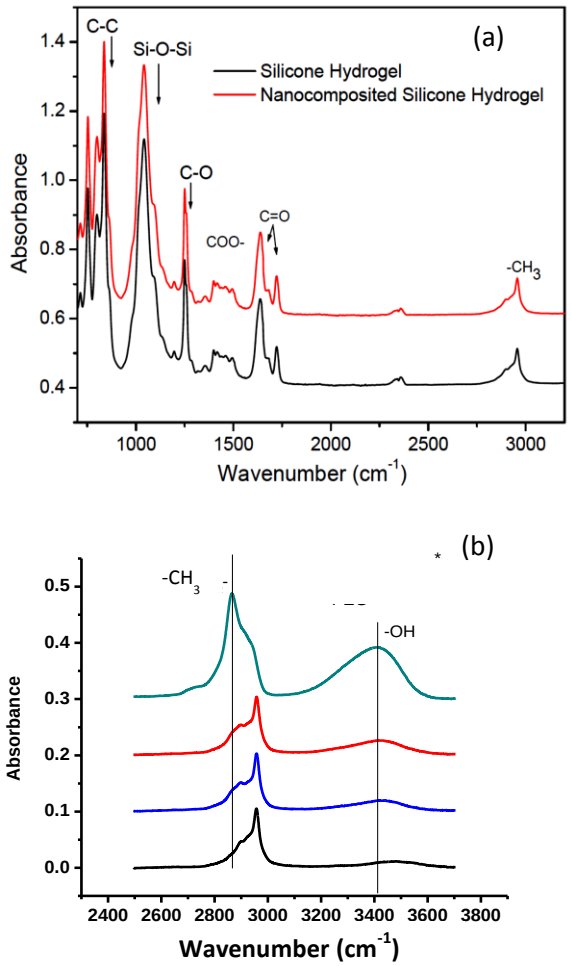

Figure 5. (a) FTIR spectra of silicone and nanocomposited silicone hydrogel. (b) FTIR spectra of PEG and nanocomposited silicone hydrogel. (—) pure PEG; (—) nanocomposited silicone hydrogel; (—) nanocomposited silicone hydrogel modified by MAPLE-deposited PEG; (—) nanocomposited silicone hydrogel modified by dip-coated PEG.

hydrogel is 16±2% less than that on silicone hydrogel. The BSA adsorption on PEG deposited nanocomposited silicone hydrogels is decreased over 40±2% in comparison with that on silicone hydrogel without PEG. The BSA adsorption is further reduced with more PEG deposited on the surface of nanocomposited silicone hydrogel.

BSA, a globular protein, can be described as having a densely packed hydrophobic core surrounded by a hydrophilic coat of polar amino acids. Based on previous reports,[35-36] when BSA interact with a hydrophobic surface. The hydrophobic core of BSA became less organized to achieve a more energetically favourable state, thus entropy of the BSA adsorption on silicone hydrogel increases. On the contrary, the protein adsorption on hydrophilic surfaces, such as nanocomposited silicone hydrogel with PEG deposition, has less entropic gain. In addition, the lower electrostatic interaction between BSA and PEG deposited on the

nanocomposited silicone hydrogel inhibits the BSA adsorption of the nanocomposited silicone hydrogel.[37]

The antimicrobial efficiency of nanocomposited silicone hydrogel with and without PEG coating to both *S. auerus* and

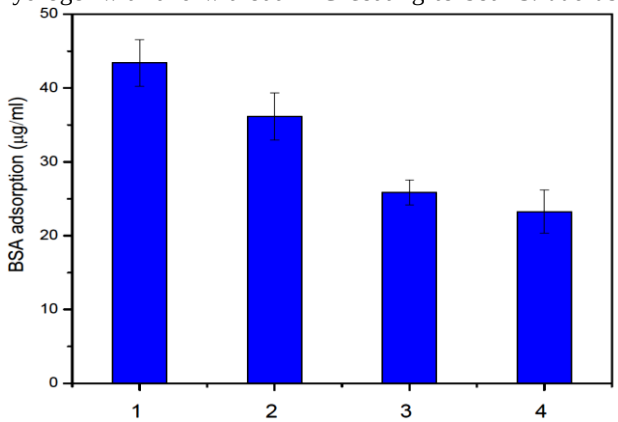

Figure 6. BSA adsorption of silicone and nanocomposited silicone hydrogels with/without PEG deposition by MAPLE (t =2hr). Here, 1- silicone hydrogel; 2- nanocomposited silicone hydrogel; 3- PEG deposited on nancomposited silicone hydrogel (t = 1hr); 4- PEG deposited on nancomposited silicone hydrogel (t = 2hr).

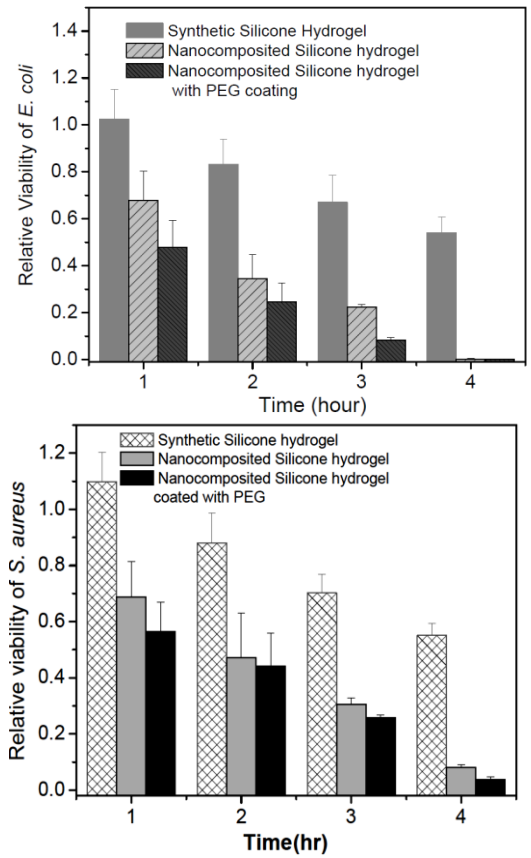

Figure7. Antimicrobial efficiency of silicone hydrogel and nanocomposited silicone hydrogel with/without PEG coating to (a) *E. coli* (b) *S. auerus,*

E. coli were evaluated quantitatively though the drop-test method, respectively. Figure 7a and Figure 7b clearly indicate that nanocomposited silicone hydrogel with PEG coating is able to significantly reduce the amount of *E. coli* and *S. auerus* on the surface of samples at the first hour of the drop-test. There are very few living bacteria left on both nanocompoisted silicone hydroges with and without PEG coating after 4 hours of the drop-test. Whereas the relative viability of *E.coli* and *S. auerus* is 0.56±0.05 and 0.54±0.07, respectively, after 4 hours of drop test.

We further studied the bacterial growth on both of the commercialized urology catheters stent made of silicone, and the nanocomposited silicone with PEG modification (t = 2hr). The results indicate that nanocomposited silicone hydrogel with PEG can reduce the viability of *E.coli* almost an order of magnitude, i.e. from $1.20x10^6$ CFU/cm^2 to $3.69x10^5$ CFU/cm^2 compared to the silicone Foley catheter,. The data have a p value smaller than 0.05 for single-tail Student T-Test, and a p value slightly higher than 0.05 for double-tail Student T-test.

Cytotoxicity of nanocomposited silicone hydrogels

Biocompatibility of the silicone hydrogel and the nanocomposited silicone hydrogel was assessed by using NIH/3T3 mouse fibroblast cells. Samples were immersed in culture medium and incubated with cells for 24 h. Figure 8 indicates the relative cell viability of different samples are higher than 80% after 24 h; thus silicone hydrogels and

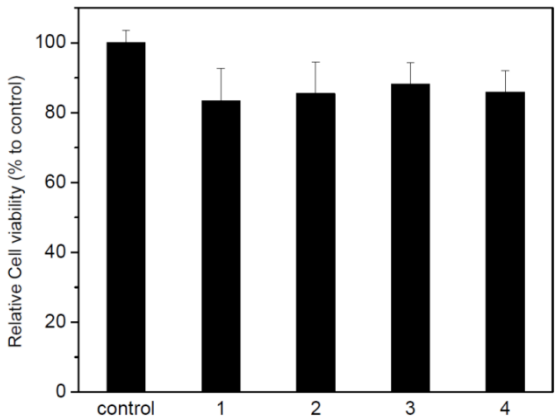

Figure 8. Relative cell viability (%) of silicone samples. 1- silicone hydrogel; 2- nanocomposited silicone hydrogel; 3- PEG deposited on the nancomposited silicone hydrogel (t = 1hr); 4- PEG deposited on the nancomposited silicone hydrogel (t = 2hr).

nanocomposited silicone hydrogels with/without PEG deposition have no significant toxic effects to mouse NIH/3T3 cells.

Conclusions

Nanocomposited silicone hydrogel by incorporating SiO_2 NPs was made through photo-polymerization. The inorganic nanostructures are homogeneously dispersed in silicone hydrogel, which increases the Young's modulus by 12.9% in comparison with the silicone hydrogel. The hydrophility of nanocomposited silicone hydrogel is improved as well which reflects the enhanced swelling behaviour. A matrix-assisted pulsed laser evaporation (MAPLE) with a pulsed Nd:YAG Laser at 532 nm was applied in depositing (PEG) molecules on

the surface of nanocomposited silicone hydrogels to improve the hydrophobicity of silicone hydrogels. The AFM topographies of the nanocomposited silicone hydrogels with PEG deposition show micro-islands of PEG which increase with increasing irradiation time (*t*). Compared to silicone hydrogel, a significant decrease (> 40±2 %) in protein adsorption is observed when PEG molecules were deposited on the nanocomposited silicone hydrogel when t = 2 h. As compared to that of the commercial silicone catheter, the growth of bacteria on the nanocomposited silicone hydrogel with PEG surface modification reduces from $1.20x10^6$ CFU/cm^2 to $3.69x10^5$ CFU/cm^2, almost an order of magnitude. In addition, the relative cell viabilities of NIH/3T3 mouse fibroblast cells treated with the nanocomposited silicone hydrogels with/without PEG deposition were studied. No significant toxic effect is imposed on the cells. The results indicate that MAPLE process is a controllable and contamination-free technique to modify the surface of silicone hydrogels. Meanwhile, it is noted that it is a challenge to design a surface to reject the growth of all types of bacteria.

Acknowledgements

We would like to acknowledge the Natural Science and Engineering Research Council of Canada (NSERC) and the Canada Foundation for Innovation (CFI) for financial support.

Notes and references

[1]Department of Chemical and Biochemical Engineering, University of Western Ontario, London, N6A 5B9, Canada
[2]Department of Medical Biophysics, University of Western Ontario, London, N6A 3K7, Canada
[3]Department of Surgery in the Schulich School of Medicine & Dentistry, , University of Western Ontario, London, N6A 3K7, Canada

1 G. Reid, J. D. Denstedt, Y. Kang, D. Lam, and C. Nause, *J. Urol.*, 1992, **148**,1592.
2 G. L. Shaw, S. K. Choong, and C. Fry, *Urol. Res*., 2005, **33**, 17.
3 A. G. Gristina, *Science*, 1987, **237**, 1588.
4 P. F. Keane, M. C. Bonner, S. R. Johnston, A. Zafar, and S. P. Gorman, *Br. J. Urol.*, 1994, **73**, 687.
5 M. Wilson, *Sci. Prog*., 2001, **84**, 235.
6 D. B. Hall, P. Underhill, and J. M. Torkelson, *Polym. Eng. Sci.*, 1998, **38**, 2039.
7 L. Jones, V. Franklin, K. Evans, R. Sariri, and B. Tighe, *Optom. Vis. Sci.*, 1996, **73**, 16.
8 O. Wichterle, and D. Lim, *Nature*, 1960, **185**, 117.
9 L. Jones, M. Senchyna, M. A. Glasier, J. Schickler, I. Forbes, D. Louie, and C. May, *Eye Contact Lens*, 2003, **29**, S75.
10 J. S. Olsen, C. Brown, C. C. Capule, M. Rubinshtein, T. M. Doran, R. K. Srivastava, C. Feng, B. L. Nilsson, J. Yang, and S. Dewhurst, *J. Biol. Chem*., 2010, **285**, 35488.
11 M. Kobayashi, Y. Terayama, H. Yamaguchi, M. Terada, D. Murakami, K. Ishihara, and A. Takahara, *Langmuir*, 2012, **28**, 7212.
12 Y. Imai, T. Ogoshi, K. Naka, and Y. Chujo, *Polym. Bull*., 2000, **45**, 9.
13 B. M. Novak, and C. Davies, *Macromolecules*, 1991, **24**, 5481.
14 S. Wohlrab, A. Schönhals, H. Goering, and J. F. Friedrich, *Polym. Chem*., 2010, **1**, 1226.
15 P. M. Ajayan, L. S. Schadler, and P. V. Braun, in "Nanocomposite Science and Technology", Wiley VCH: Wiley, 2003.
16 S, M, Liff, N. Kumar, and G. H. McKinley, *Nat. Mater*., 2007, **6**, 76.
17 L. T. Zhuravlev, *Colloids. Surf. A*, 2000, **173**, 1.
18 A. M. Mumin, J. W. Barrett, G. A. Dekaban, and J. Zhang, *J. Colloid. Interface. Sci.*, 2011, **353**, 156.
19 P. Bures, Y. Huang, E. Oral, and N. A. Peppas, *J. Control Release*, 2001, **72**, 25.
20 N. Wisniewski and M. Reichert, *Colloids Surf. B: Biointerfaces* 2000, **18**, 197.
21 M. Ghosh, F. Fan, and K. J. Stebe, *Langmuir*, 2007, **23**, 2180.
22 A. I. Lopez, A. Kumar, M. R. Planas, Y. Li, T. V. Nguyen, and C. Cai, *Biomaterials*, 2011, **32**, 4317.
23 R. Cristescu, D. Mihaiescu, G. Socol, I. Stamatin, I. N. Mihailescu, and D. B. Chrisey, *Appl. Phys. A*, 2004, **79**, 1023.
24 Y. Guo, A. Morozov, D. Schneider, J. W. Chung, C. Zhang, M.Waldmann, N. Yao, G. Fytas, C. B. Arnold, R. D. Priestley, *Nature Mat.*, 2012, **11**, 337.
25 D. M. Bubb, A. O. Sezer, J. Gripenburg, B. Collins, and E. Brookes, *Appl. Surf. Sci.*, 2007, **253**, 6465.
26 J. Zhang, L. M. Postovit, D. Wang, R. B. Gardiner, R. Harris, A. M. Mumin, and A. A. Thomas, *Nanoscale Res. Lett*., 2009, **4**, 1297.
27 J. Kim, A. Conway, and A. Chauhan, *Biomaterials*, 2008, **29**, 2259.
28 B. Bareiss, M. Ghorbani, F. F. Li, J. A. Blake, J. C. Scaiano, J. Zhang, C. Deng, K. Merrett, J. Harden, F. Diaz-Mitoma, and M. Griffith, *the Open Tissue Eng. & Reg. Med*., 2010, **3**, 10.
29 D. R. James, A. Siemiarczuk, and W. R. Ware, *Rev. Sci. Instrum.*, 1992, **63**, 1710.
30 Lakowicz, J. Frequency-Domain Lifetime Measurements. In Principles of Fluorescence Spectroscopy; Springer US, 2006, pp 157-204.
31 S. Sun, B. Sun, W. Zhang, and D. Wang, *Bull. Mater. Sci.*, 2008, **31**, 61.
32 P. G. Agache, C. Monneur, J. L. Leveque, and J. Rigal, *Arch. Dermato. Res.*, 1980, **269**, 221.
33 B. Toftmann, K. Rodrigo, J. Schou, and R. Pedrys, *Appl. Surf. Sci*., 2005, **247**, 211.
34 I. A. Paun, A. Moldovan, C. R. Luculescub, A. Staicub, and M. Dinescub, *Appl. Surf. Sci*., 2012, **258**, 9302.
35 V. Tangpasuthadol, N. Pongchaisirikul, and V. P. Hoven, *Carbohyd. Res*., 2003, **338**, 937.
36 A. Azioune, M. M. Chehimi, B. Miksa, T. Basinska, and S. Slomkowski, *Langmuir*, 2002, **18**, 1150.
37 B. Nerli, M. Espariz, G. Picó, *Biotechnol Bioeng*., 2001, **72(4)**, 468.

Nanocomposited Silicone Hydrogels; P. Yin, *et al.*

Graphical Abstract

Compared to the commercial silicone catheters, the nanocomposited silicone hydrogel with a laser-assisted surface modification can reduce the growth of bacteria from 1.20×10^6 CFU/cm^2 to 3.69×10^5 CFU/cm^2, almost an order of magnitude.